Taylor & Francis
Taylor & Francis Group

Preparative Biochemistry & Biotechnology

ISSN: 1082-6068 (Print) 1532-2297 (Online) Journal homepage: www.tandfonline.com/journals/lpbb20

Immobilization and characterization of celery root peroxidase on multi-walled carbon nanotubes

Mehmet Doğan, Serap Doğan, Şeyma Çam, Pınar Turan Beyli, Zeynep Bicil & Berna Koçer Kızılduman

To cite this article: Mehmet Doğan, Serap Doğan, Şeyma Çam, Pınar Turan Beyli, Zeynep Bicil & Berna Koçer Kızılduman (2026) Immobilization and characterization of celery root peroxidase on multi-walled carbon nanotubes, Preparative Biochemistry & Biotechnology, 56:3, 395-408, DOI: 10.1080/10826068.2025.2543282

To link to this article: https://doi.org/10.1080/10826068.2025.2543282

PREPARATIVE BIOCHEMISTRY & BIOTECHNOLOGY
2026, VOL. 56, NO. 3, 395–408
https://doi.org/10.1080/10826068.2025.2543282

Taylor & Francis
Taylor & Francis Group

Immobilization and characterization of celery root peroxidase on multi-walled carbon nanotubes

Mehmet Doğan[a], Serap Doğan[b], Şeyma Çam[a], Pınar Turan Beyli[a], Zeynep Bicil[a] and Berna Koçer Kızılduman[a]

[a]Faculty of Science and Literature Department of Chemistry, Balikesir University, Balikesir, Turkey; [b]Faculty of Science and Literature Department of Molecular Biology and Genetics, Balikesir University, Balikesir, Turkey

ABSTRACT

This study investigates the immobilization of peroxidase (POD) concentrated from celery root onto multi-walled carbon nanotubes (MWCNTs), focusing on its effects on enzymatic activity, stability, and reusability. POD was extracted using phosphate buffer, followed by ammonium sulfate precipitation and dialysis. Immobilization conditions were optimized based on contact time and support amount. The immobilized enzyme showed maximum activity after 300 minutes, whereas increasing MWCNT content led to reduced activity due to diffusion limitations. Kinetic analysis revealed that immobilized POD retained a similar V_{max} compared to the free enzyme, but exhibited significantly higher K_M values. Comprehensive characterization using BET, FTIR, SEM/EDX, TGA, and TEM confirmed successful immobilization and enzyme–nanotube interactions. BET analysis showed a decrease in surface area from 275 to 197 m^2/g. FTIR spectra confirmed the appearance of protein-specific bands post-immobilization, and EDX data revealed increased nitrogen and oxygen levels, along with Fe as a cofactor marker. Thermal degradation profiles also changed, while SEM and TEM images demonstrated morphological alterations on the nanotube surfaces. Immobilized POD preserved activity at pH 4.0–6.0 and optimum temperature (30 °C), and retained functionality over multiple cycles and storage periods. These findings highlight the potential of MWCNT-supported POD systems in environmentally relevant and industrial biocatalytic applications.

KEYWORDS

Carbon nanotube; celery root; characterization; immobilization; peroxidase

Introduction

Enzymes are protein-based molecules that act as biocatalysts, accelerating various biochemical reactions. However, free enzymes are very sensitive to environmental conditions and their lifespan may be limited. To enable the economic and sustainable use of enzymes in industrial applications, enzyme immobilization has been developed as a key method.[1,2] Enzyme immobilization, while offering substantial benefits, also presents certain limitations that may affect its practical implementation. Specifically, the complexity and high cost of immobilization processes can pose economic challenges for industrial-scale applications. Structural alterations in the enzyme's active site during immobilization and incompatibility with support materials may lead to decreased catalytic activity.[3,4] Furthermore, immobilization conditions and the nature of the enzyme–support interactions can influence performance, while environmental parameters such as pH shifts may exacerbate activity losses.[4,5] Traditional methods often suffer from enzyme leakage, restricted molecular mobility, and low activity retention, prompting the development of advanced strategies such as "immobilized but not rigid" approaches.[6] In nanoscale systems like enzyme@MOF particles, recovery difficulties and activity losses upon reuse have also been reported, leading to suggestions for using micron-sized alternatives to improve reusability.[7] Additionally, some nanostructured supports may exhibit limited mechanical strength and adversely affect enzyme stability, posing challenges to long-term sustainability.[5] Nevertheless, despite these drawbacks, enzyme immobilization remains a valuable strategy due to its ability to enhance catalytic efficiency, extend enzyme lifespan, and enable repeated use in industrial settings. Enzyme immobilization refers to the stabilization of enzymes by anchoring them onto a solid support matrix instead of allowing them to remain freely in solution. This approach enhances the reusability of enzymes, improves their thermal and chemical stability, and reduces the overall cost of industrial processes.[1,2] Owing to these advantages, enzyme immobilization has found extensive applications across various sectors including food, pharmaceuticals, biofuels, environmental technologies, and textiles. Immobilized enzymes play a crucial role in processes such as lactose hydrolysis in the food industry, the use of stereoselective biocatalysts in pharmaceutical production, the degradation of lignocellulosic biomass in biofuel generation, and the removal of toxic compounds from wastewater in environmental biotechnology. They are also of

CONTACT Mehmet Doğan mdogan@balikesir.edu.tr, mdogan7979@gmail.com Faculty of Science and Literature Department of Chemistry, Balikesir University, Balikesir, Turkey.

critical importance in fields such as antioxidant activity determination and biosensor development. Among the numerous industrially relevant enzyme classes, peroxidases (POD), which belong to the oxidoreductase group, have attracted significant attention. PODs are enzymes capable of oxidizing a variety of organic and inorganic compounds by using peroxides such as hydrogen peroxide (H_2O_2) as substrates. These enzymes can be derived from diverse biological sources including plants, animals, and microorganisms. The catalytic activity of PODs makes them suitable for various applications in environmental, food, and health-related sectors.[8] In environmental applications, PODs are effectively used in the degradation of phenolic compounds, aromatic pollutants, dyes, and pesticides. Their utilization has become widespread in the oxidative degradation of toxic phenolic waste in wastewater treatment, quality control in the food industry, and detection of target molecules in biosensors. The broad applicability of PODs has drawn growing interest in recent years, particularly due to their contributions to environmental sustainability and green chemistry approaches.

Various organic, inorganic, polymeric, and nanostructured supports have been employed for the immobilization of PODs in the literature, including nylon-6,[9] magnetite-modified polyaniline (PANImG),[10] polyaniline (PANI),[11] aminopropyl glass beads,[12,13] polyvinyl alcohol (PVA),[14] polystyrene microplates (MaxiSorp™),[15] natural carriers and binders,[16] natural support materials,[17] chitosan nanoparticles,[18] activated wool,[19] Fe_3O_4 magnetic nanoparticles,[20] modified chitosan beads,[21] titanate nanowires,[22] cinnamic carbohydrate esters,[23] the metal-organic framework Hf-DBA,[24] and lysine-functionalized gum arabic-coated iron oxide nanoparticles.[25] These supports have significantly improved the activity, stability, and reusability potential of the enzyme. In recent years, carbon-based nanomaterials, particularly multi-walled carbon nanotubes (MWCNTs), have been introduced for enzyme immobilization, though studies in this area remain limited. MWCNTs are tubular structures formed by rolling graphene sheets into single- or multi-walled cylindrical shapes.[26,27] Jun et al.[28] immobilized Jicama peroxidase onto a composite membrane made of MWCNTs and polyvinyl alcohol (PVA) through covalent bonding using glutaraldehyde and developed an optimized model for this process. The results indicated that the immobilized enzyme achieved a high loading capacity with an efficiency of 81.74% and exhibited significantly improved stability under varying pH, temperature, and storage conditions compared to the free enzyme.[28] Kim et al.[15] immobilized horseradish POD onto MWCNTs and evaluated the protein binding capacity of the matrix and the enzyme activity under various pH and high-temperature conditions. Their findings showed that the activity of horseradish POD immobilized on MWCNTs was preserved and increased proportionally with its initial concentration, and that MWCNTs exhibited a higher protein binding capacity than polystyrene microplates.[15] Lee et al.[29] optimized the immobilization of horseradish POD onto carboxylated MWCNTs and examined changes in enzyme activity. It was found that the immobilized horseradish POD displayed a broader activity range between pH 4–9 compared to its free counterpart.[29] Li et al.[30] developed a novel composite support using MWCNTs and cordierite matrix to enhance the efficiency of horseradish POD in wastewater treatment. Experimentally, the immobilized enzymes showed higher activity than the free enzymes, and horseradish POD activity increased with the MWCNT content. Moreover, the immobilization process conferred greater stability against temperature and pH variations, thereby improving the overall performance.[30] These studies demonstrate that immobilized enzymes can be employed more reliably and durably in industrial applications.

In the literature, PODs have been isolated from celery root and their kinetic properties have been investigated. However, to ensure wider and more stable industrial use of this enzyme, immobilization is necessary. To date, there is no reported study on the immobilization of POD extracted from celery root. Within this context, the present study aimed to immobilize POD enzyme, concentrated from celery root using phosphate buffer extraction, ammonium sulfate precipitation, and dialysis, onto the surface of MWCNTs. The primary objective of this study is to investigate the effects of immobilization on the catalytic activity, stability, and reusability of peroxidase. Furthermore, MWCNT and POD-immobilized MWCNT samples were characterized using Brunauer–Emmett–Teller (BET) surface area analysis, Fourier-transform infrared spectroscopy (FTIR), scanning electron microscopy/energy-dispersive X-ray spectroscopy (SEM/EDX), thermogravimetric analysis (TGA), and transmission electron microscopy (TEM). The ultimate aim of this study is to enhance the applicability of the immobilized enzyme system in potential environmental and biotechnological applications. The findings are expected to contribute to the advancement of immobilized enzyme technologies, particularly those based on nanomaterial-supported biocatalyst systems.

Materials and methods

Materials

All chemicals used in this study were of analytical grade and used without further purification. MWCNTs (purity 96%, outside diameter 8–18 nm, inside diameter 5–10 nm, specifice surface area 220 m^2/g) were purchased from Nanografi (Ankara, Türkiye). Celery root, which served as the source of POD enzyme, was obtained from a local market in Balıkesir, Türkiye.

Preparation of MWCNTs

A mixture of 10 g MWCNT and 200 mL of 5 M HCl solution (IsoLab Chemicals, 37%) was placed in a 500 mL round-bottom flask and sonicated at 30 °C for 2 hours. The mixture was then refluxed at 70 °C for 48 hours. After refluxing, the mixture was again sonicated for 1 hour. Subsequently, 500 mL of deionized water was added to dilute the mixture. The diluted suspension was filtered using a vacuum filtration apparatus and washed with plenty of water until neutral pH (pH 7) was achieved. The purified MWCNTs were dried in an oven at 60 °C for 24 hours, followed by vacuum drying at the same temperature.[31]

Extraction and concentration of peroxidase enzyme

The extraction and experimental procedures for POD were adapted from the method described by Sakharov et al.[32] Prior to extraction, celery roots were treated with liquid nitrogen to disrupt cellulose fibers. For enzyme extraction, 20 g of nitrogen-treated celery root tissue was homogenized in a Waring Blender with 50 mL of 0.1 M phosphate buffer (pH 6.5) containing 28 mM ascorbic acid, 5 mM EDTA, and 5% NaCl for 2 minutes. The extract was filtered through cheesecloth, and the filtrate was centrifuged at 15,000 × g for 10 minutes at 4 °C.

The crude plant extract was brought to 70% saturation with ammonium sulfate using the following formula, and the precipitated POD was collected by centrifugation at 15,000 × g for 30 minutes:

$$g_{[(NH_4)_2SO_4]} = \frac{1.77V(S_2 - S_1)}{3.54 - S_2}$$

where V is the volume of the upper phase, S_1 is the initial ammonium sulfate saturation, and S_2 is the desired saturation level.[33]

The solid precipitate obtained from ammonium sulfate precipitation was dissolved in 0.1 M phosphate buffer (pH 6.5), then dialyzed against 0.05 M phosphate buffer (pH 6.5) for 2 days with three buffer changes.[34]

Determination of enzyme activity

The peroxidase activity was determined spectrophotometrically using 2,2′-azino-bis(3-ethylbenzothiazoline-6-sulfonic acid) (ABTS) as the chromogenic substrate, based on the method described by Gallati[35] with slight modifications. The assay mixture contained 2.2 mL of 0.1 M acetate-phosphate buffer (pH 4.5), 0.6 mL of 0.01 M ABTS, 0.1 mL of hydrogen peroxide (H_2O_2), and 0.1 mL of enzyme solution (free or immobilized). The reaction was carried out at in a quartz cuvette with a path length of 1 cm. The increase in absorbance at 414 nm was monitored every 5 seconds for 2 minutes using a PerkinElmer Lambda 25 UV-Vis spectrophotometer. One unit of peroxidase activity (EU) was defined as the amount of enzyme that causes a change in absorbance of 1.0 per minute at 414 nm under the assay conditions. All activity measurements were performed in triplicate, and results were expressed as EU/mL·min.

Characterization of free enzyme

The optimum pH for celery root POD activity was determined at 25 °C using 0.1 M acetate buffer (pH 2.0–6.0) and 0.1 M phosphate buffer (pH 6.0–9.0). The pH values of buffer solutions were adjusted with 0.1 M NaOH or 0.1 M HCl. Enzyme activity was measured at 414 nm using a PerkinElmer Lambda 25 UV-Vis spectrophotometer with ABTS (0.01 M) as the substrate. The reaction was monitored by taking readings every 5 seconds for 2 minutes. The cuvette contained 2.2 mL buffer, 0.1 mL H_2O_2, 0.1 mL enzyme solution, and 0.6 mL substrate solution.[34]

The effect of temperature on enzyme activity was evaluated between 10–60 °C at the optimum pH using ABTS as the substrate. Reaction mixtures (buffer, H_2O_2, and substrate) were preheated to the desired temperatures using a Beckmann Peltier temperature controller integrated with the spectrophotometer's cell holder. Once thermal equilibrium was achieved, enzyme was added and the reaction was monitored spectrophotometrically at fixed time intervals. The reaction mixture consisted of 0.6 mL of 0.01 M substrate, 2.2 mL of 0.1 M buffer, 0.1 mL H_2O_2, and 0.1 mL enzyme solution.[36]

Enzyme kinetics were studied at optimum pH and temperature using varying substrate concentrations (0.00033–0.003 M) with a fixed amount of enzyme (0.1 mL). Michaelis–Menten constants (K_M and V_{max}) for ABTS were calculated from the Lineweaver-Burk plot of 1/V versus 1/[S].

Immobilization of POD onto MWCNTs

To determine the optimal contact time for immobilization, 10 mL of phosphate extraction buffer was added to test tubes containing 0.05 g of MWCNT. The tubes were incubated at 25 °C and shaken at 200 rpm. At predetermined time intervals (0–450 min), tubes were centrifuged, and the supernatants were collected for activity measurement. The residual solid was washed twice with 10 mL phosphate buffer, and the washed supernatants were also centrifuged. Then, 0.05 g of the washed solid residue was taken from each sample to determine enzyme activity. ABTS was used as the substrate.[37]

Various amounts of MWCNT (0.05, 0.1, 0.15, 0.2, 0.25, and 0.3 g) were weighed into separate test tubes, each containing 5 mL phosphate extraction buffer. The mixtures were shaken at 25 °C and 200 rpm for 2 hours. After the optimized contact time, the mixtures were centrifuged and the supernatant was filtered using a syringe filter (0.45 µm pore size) for enzyme activity analysis. The activity of the immobilized enzyme on the solid phase was determined after washing.[37] ABTS was used as the substrate in all activity assays.

Optimum pH, temperature, and kinetic experiments for immobilized POD were performed using the same procedures as for the free enzyme, with ABTS as the substrate.

Characterization of pristine and POD-immobilized MWCNTs

BET surface area and pore volume analyses of MWCNT and POD-immobilized MWCNT were conducted using a Quantochrome Nova2200e gas analyzer. Samples were degassed at 100 °C for 24 hours prior to analysis.

FTIR-ATR spectra of MWCNT and POD-immobilized MWCNT were obtained using a PerkinElmer Spectrum 100 spectrometer.

DTA/TG thermograms of MWCNT and POD-immobilized MWCNT were recorded under a nitrogen atmosphere at a heating rate of 20 °C/min from 30 °C to 1000 °C.

TEM images of MWCNT were obtained using a Hitachi HT7800 microscope operated at an acceleration voltage of 100 kV.

SEM images of MWCNT and POD-immobilized MWCNT samples were acquired using a Zeiss EVO LS 10 microscope, and EDX analysis was performed using a Bruker EDX detector at 20 kV acceleration voltage.

The flow diagram presented in Figure 1 illustrates the purification steps, kinetic properties, and characterization processes of free and immobilized enzymes.

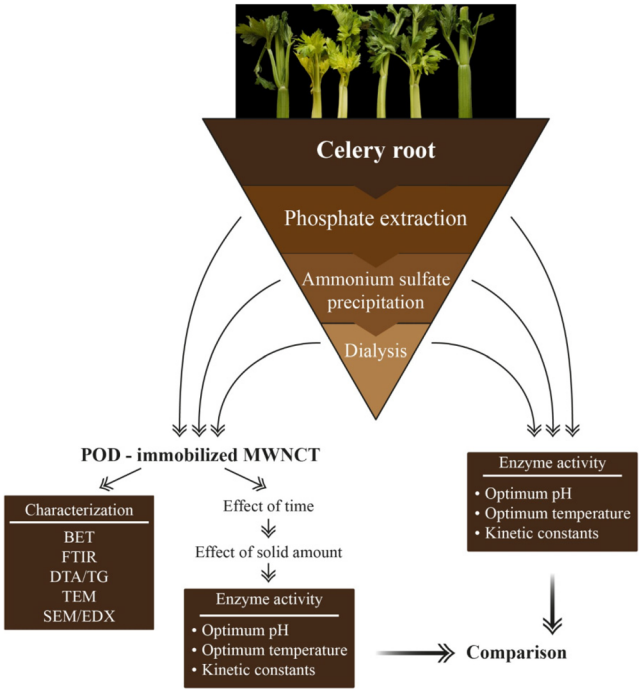

Figure 1. Flow diagram of the study.

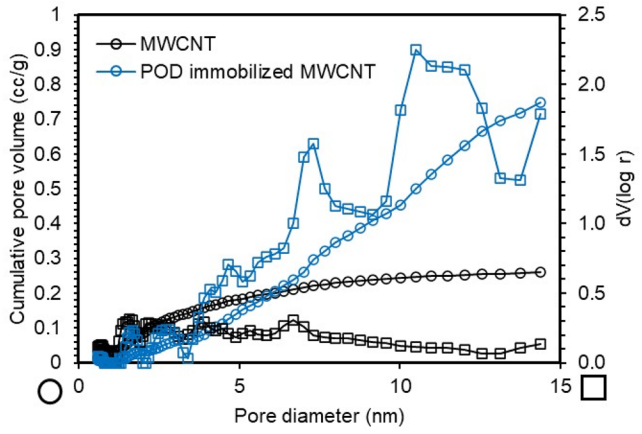

Figure 2. The changing of cumulative pore volumes of MWCNTs and POD-immobilized MWCNTs versus pore diameters.

Results and discussion

Characterization of pristine and POD-immobilized MWCNTs

BET surface area is a measurement used to determine the surface area of a material and is particularly significant in applications involving porous materials, activated carbon, immobilization processes, and catalysts. Immobilization involves the binding of biomolecules (e.g., enzymes, antibodies) or other active components onto a support material. A high BET surface area indicates a greater available active surface, thereby allowing more biomolecules to be immobilized. This enhances the functional efficiency of the immobilized components. Figure 2 presents the pore diameter versus cumulative pore volume plots for both MWCNT and POD-immobilized MWCNT samples. Additionally, the pore volumes and BET surface areas calculated using the DFT (Density Functional Theory) method are provided in Table 1. The BET surface area of pristine MWCNT was measured as 275 m^2/g, which decreased to 197 m^2/g following POD immobilization. This reduction indicates a decrease in surface area due to the immobilization process. The observed decrease may be attributed to the coverage of the tube ends and surfaces of MWCNTs by the POD enzyme.[38] Furthermore, Table 1 displays the pore volume values for both MWCNT and enzyme-immobilized samples. The data suggest that the samples predominantly consist of mesopores, with negligible presence of micropores. In this case, it can be said that the pore diameters of MWCNTs vary in the range of 2-15 nm and they create a suitable immobilization environment for enzymes.[39]

The FTIR spectra of MWCNT and POD-immobilized MWCNTs are presented in Figure 3. Significant spectral changes were observed in the FTIR spectrum of MWCNT after the immobilization process. The spectrum of pristine MWCNT exhibits no characteristic bands corresponding to functional groups, except for a band at 1565 cm^{-1}, which is attributed to the C=C stretching vibrations indicative of the graphene structure. In contrast, the FTIR spectrum of the POD-immobilized MWCNT displays several new bands. The broad band at 3401 cm^{-1} corresponds to O–H stretching vibrations, indicating the presence of hydroxyl groups associated with hydrogen bonding. The bands at 2927 and 2855 cm^{-1} are attributed to the stretching vibrations of C–H bonds, typically arising from aliphatic groups. The band observed at 1701 cm^{-1} is characteristic of carbonyl (C=O) groups, suggesting the presence of peptide bonds or other carbonyl-containing compounds. The band at 1523 cm^{-1} is associated with secondary amide groups and is considered an indicator of the secondary structure of proteins. This band results from N–H bending and C–N stretching vibrations and provides insight into the stability of the protein

Table 1. BET surface area and pore volume data of MWCNT and POD-immobilized MWCNTs.

Samples	S_{BET} (m^2/g)	V_t (cc/g)	V_{micro} (cc/g)	V_{meso} (cc/g)	V_{macro} (cc/g)
MWCNT	275	0.410	–	0.360	0.050
POD-immobilized MWCNT	197	1.139	–	0.877	0.262

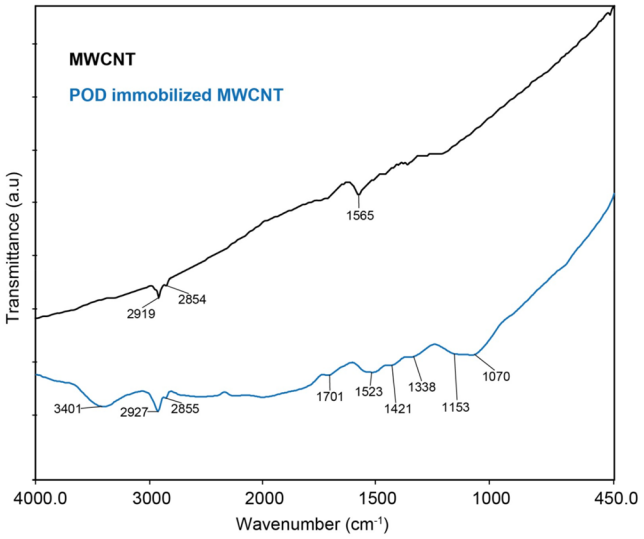

Figure 3. FTIR spectra of MWCNT and POD immobilized MWCNTs.

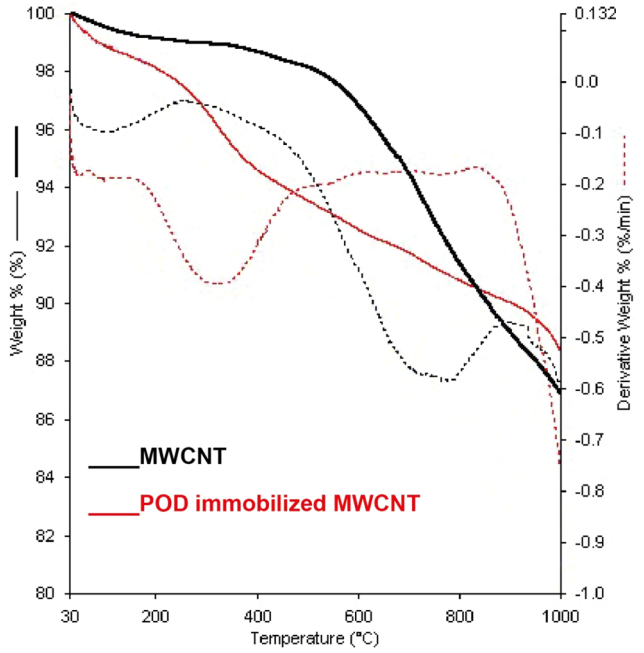

Figure 4. Thermograms of MWCNT and POD immobilized MWCNTs.

Table 2. Thermal stability data of MWCNT and POD immobilized MWCNTs.

Samples	T_{max1} (°C)	DeltaY$_1$ (%)	T_{max2} (°C)	DeltaY$_2$ (%)	T_{max3} (°C)	DeltaY$_3$ (%)	Residue (%)
MWCNT	64	1.0	--	--	863	10.2	86.9
POD immobilized MWCNT	65	1.2	319	4.9	658	2.8	88.3

structure in the enzyme. The band at 1421 cm^{-1} is generally related to CH_2 groups, indicating the presence of aliphatic side chains within the protein structure. The band at 1338 cm^{-1} corresponds to C–N stretching vibrations and signifies the presence of amide groups in the protein structure. Finally, the band at 1070 cm^{-1} is assigned to C–O stretching vibrations and is commonly associated with carbohydrates or glycosidic components. These FTIR bands collectively confirm the successful immobilization of the POD enzyme onto the surface of MWCNTs.[40]

DTA/TG is an analytical method used to study the thermal properties of materials. This method provides important information to understand the behavior of materials against heat and their physical or chemical changes. Figure 4 presents the thermograms of MWCNT and POD-immobilized MWCNTs. The thermal stability parameters derived from these thermograms are summarized in Table 2. In the thermogram of MWCNT, mass losses are observed at 64 °C and 863 °C. The 1% mass loss at 64 °C is likely due to the evaporation of moisture within the MWCNT structure. The 10.2% mass loss at 863 °C is attributed to the decomposition of the carbon nanotube framework.[41,42] These results indicate that MWCNT undergoes single-step degradation with a total mass loss of 13.1%. In contrast, the thermogram of POD-immobilized MWCNT exhibits three distinct stages of mass loss. The first, a 1.1% mass loss at 65 °C, is likely due to the removal of moisture and minor impurities. The second, 4.9% mass loss at 319 °C, is due to the removal of functional groups from the structure of POD immobilized MWCNT. The third, 2.8% mass loss at 658 °C, is due to the degradation of the structure of MWCNT. From the thermograms, it can be inferred that while MWCNT undergoes degradation in a single step, the immobilized sample degrades in two distinct stages. Furthermore, it is observed that the thermal stability of MWCNT decreases with immobilization. A similar thermal degradation behavior has been reported for the immobilization of L-asparaginase enzyme onto the surface of MWCNTs.[43] According to thermogravimetric analysis (TGA) data, pristine MWCNT exhibited a single-step degradation profile around 800 °C due to the absence of moisture and organic impurities. In contrast, the L-asparaginase/MWCNT composite showed a two-step mass loss pattern. The first degradation stage occurred at approximately 250 °C, corresponding to the thermal decomposition of the L-asparaginase enzyme. The second stage, observed around 700 °C, was attributed to the breakdown of the carbon nanotube matrix. The shift of the MWCNT degradation temperature from 800 °C to 700 °C upon enzyme immobilization indicates a noticeable reduction in the thermal stability of the nanotube structure. This two-step degradation behavior clearly demonstrates the influence of enzyme immobilization on the thermal properties of the composite material.

SEM/EDX is a technique employed to examine the structural and surface characteristics of carbon nanotubes (CNTs) and enzyme-immobilized CNTs. It also provides insights into their functional properties, elemental composition, and, notably, the presence of cofactor metals that indicate successful enzyme immobilization. Figure 5 presents the SEM images of MWCNT and POD-immobilized MWCNTs. It is evident that enzyme immobilization induces significant morphological changes in the MWCNT structure. SEM images of MWCNTs display an agglomerated structure composed of overlapping carbon nanotubes with distinct intertubular spacing. This agglomeration is attributed to van der Waals interactions between individual nanotubes. In contrast, after immobilization, the surface of MWCNTs appears to be

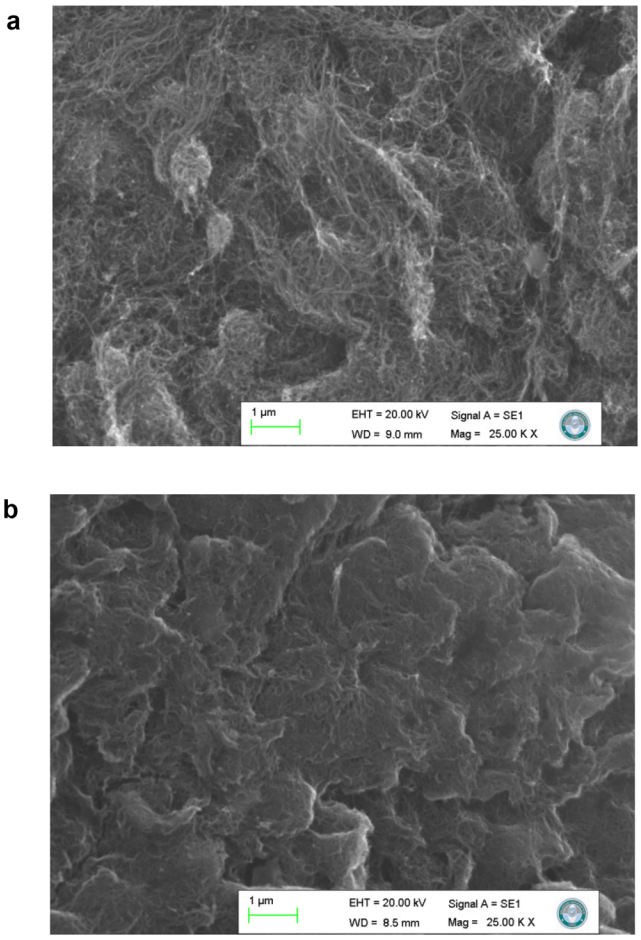

Figure 5. SEM images of (a) MWCNT and (b) POD immobilized MWCNTs.

coated with enzyme molecules, and the agglomerated domains are more delineated by defined interfacial boundaries. These morphological changes suggest that the enzyme molecules are physically adsorbed onto the surfaces of the carbon nanotubes. Furthermore, while the typical cylindrical morphology of CNTs is preserved, slight bulges or denser regions are observed at sites where enzymes are bound.

The EDX spectra and elemental mapping images of the samples are shown in Figure 6, and their corresponding elemental compositions are listed in Table 3. The EDX analysis of MWCNT indicates a composition of 91.12% carbon, 4.13% oxygen, and a total of 4.75% of other elements including Na, Al, N, Cl, P, and Fe. SEM images of both MWCNT and POD-immobilized MWCNTs were acquired under identical conditions. Since the immobilization was conducted in phosphate buffer, MWCNT was also incubated in the same buffer, then dried prior to analysis. The presence of non-carbon elements in the EDX spectrum of MWCNT can be attributed to this treatment. Following POD immobilization, the carbon content of MWCNT decreases, while oxygen and nitrogen contents increase, consistent with the presence of protein molecules. Moreover, the EDX spectrum of the POD-immobilized sample confirms the presence of Fe, which serves as a cofactor of the POD enzyme.[44] Elemental mapping further reveals that this cofactor metal is homogeneously distributed across the sample surface. These results collectively indicate that enzyme immobilization alters both the morphology and the elemental composition of MWCNTs.

TEM images of MWCNT samples at various magnification ratios are presented in Figure 7. In particular, Figure 7b clearly reveals the cylindrical structures of MWCNTs composed of 5–10 concentric layers. This figure demonstrates that each nanotube is formed by the orderly stacking of concentric graphene sheets, highlighting the atomic-level internal structure of the nanotubes. When both images are examined, the outer layers are more pronounced, while the inner layers appear less distinct; nevertheless, the interlayer spaces are visible. In the TEM image shown in Figure 7b, the outer diameter of the MWCNTs is observed to range around 14.6 ± 2.6 nm, while the inner diameter ranges around 7.3 ± 1.2 nm. The tube lengths, as previously described based on SEM images, are in the micrometer scale. Figure 7a further indicates that the diameters of the MWCNTs are different from each other. Both images confirm the multilayered and tubular structure of MWCNTs. Additionally, the MWCNTs appear to be somewhat separated from each other and distributed at a certain distance, indicating reduced aggregation.

Effect of immobilization time and solid content on POD activity

The following section presents the findings related to the activity of POD immobilized on the surface of MWCNTs, including its variation with time and solid content. It then compares the optimal pH, temperature, and kinetic parameters for both free and immobilized enzyme forms.

Immobilization refers to the process of attaching an enzyme to a solid surface or embedding it within a matrix. This approach often enhances enzyme stability and facilitates its reuse. However, the activity of immobilized enzymes may vary with time. Figure 8 illustrates the change in immobilized POD activity with time at a constant solid content. Initially, the enzyme activity increases with time, reaching a maximum rate at 300 minutes, followed by a gradual decrease. There are several possible explanations for the initial increase in immobilized enzyme activity. Immobilized enzyme activity generally increases after immobilization due to factors such as improve of the active site, more efficient substrate interaction, and surface restructuring.[45,46] Structural or configurational adjustments at the active site may occur upon immobilization due to physical or chemical interactions, potentially increasing catalytic efficiency. In some cases, these rearrangements allow the enzyme's active sites to interact more effectively with substrates. Furthermore, when enzymes are bound to a matrix or surface, they may initially struggle to interact with substrates until they reach an optimal conformation. As enzymes gradually attain favorable orientations, their activity increases. Over time, the immobilized enzymes may establish more effective interactions with the substrates, transitioning from initially low activity to a higher and more stable state. This improvement stems from the enzyme's ability to adapt to the immobilization environment and optimize its active conformation and binding orientation. As seen in the figure, enzyme activity peaks at 300 minutes and subsequently declines, with

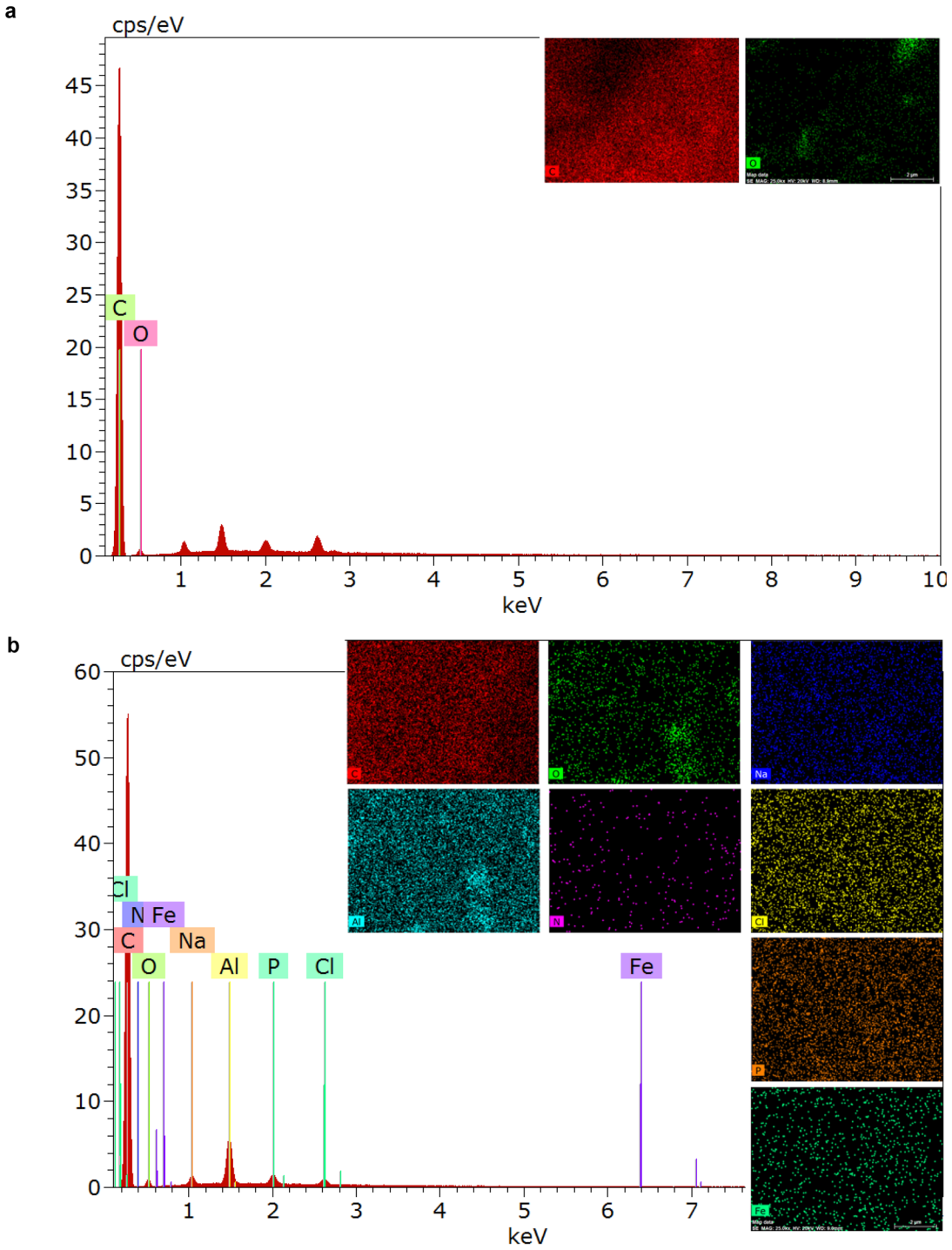

Figure 6. EDX spectra and mapping images of (a) MWCNT and (b) POD immobilized MWCNTs.

Table 3. Elemental composition of MWCNT and POD-immobilized MWCNTs.

Samples	C	O	Na	Al	N	Cl	P	Fe	Cu
MWCNT	91.12	4.13	1.08	1.50	0.36	1.05	0.67	0.09	–
POD immobilized MWCNT	88.52	5.11	0.84	2.52	1.78	0.49	0.59	0.14	–

no significant change observed beyond 330 minutes. The reduction in activity following the peak is often attributed to structural and chemical alterations occurring over time. Initially, the enzyme's active regions are more accessible; however, prolonged binding to the matrix or conformational changes at the active site may hinder substrate access. Moreover, active sites on immobilized enzymes may become blocked or obstructed with time, reducing catalytic efficiency.[47] In summary, the observed trend of increasing and then decreasing activity of immobilized enzymes can be explained by the adaptation and optimization of the enzyme structure in the early stages, followed by structural degradation, reduced surface accessibility, inhibition effects, or product accumulation. The initial increase reflects the enzyme's adaptation to its immobilized state, while the subsequent decrease is likely due to structural destabilization and environmental constraints around the enzyme.[45,48]

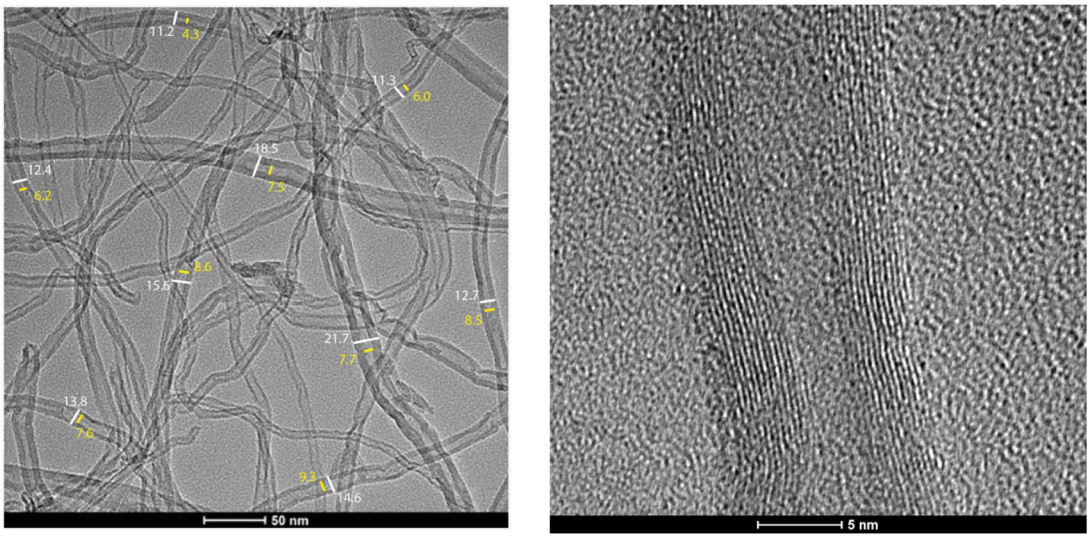

Figure 7. TEM images of MWCNT at different magnification ratios.

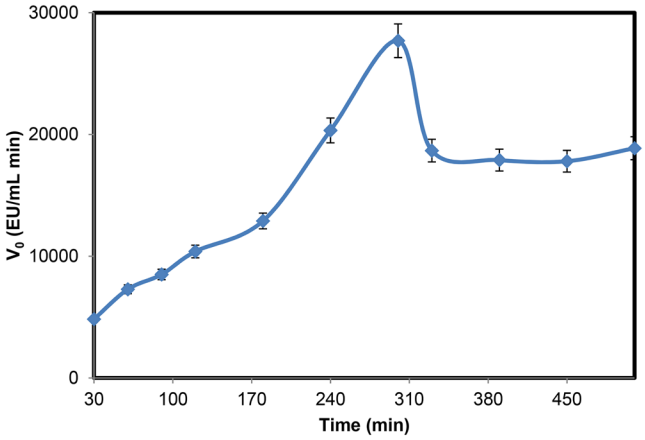

Figure 8. Effect of time to POD immobilization on the MWCNT surface.

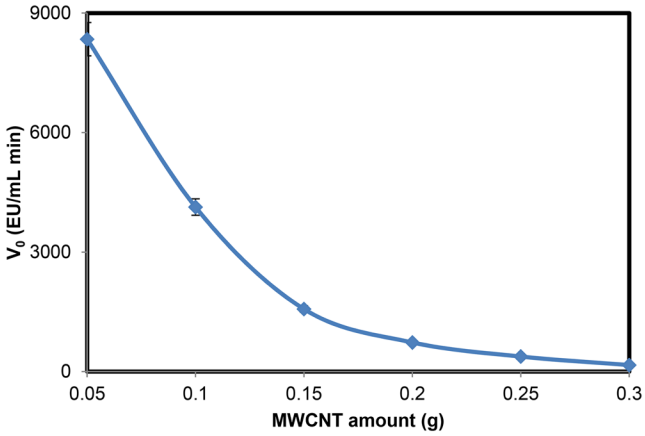

Figure 9. Effect of time to POD immobilization on the MWCNT surface.

Figure 9 illustrates the change in POD activity immobilized on the surface of MWCNTs with varying amounts of solid material. It is observed that the activity of the immobilized enzyme decreases as the amount of MWCNT increases. There are several potential reasons for this decline in immobilized enzyme activity with increasing solid content. This phenomenon is commonly observed in systems where enzymes are immobilized by binding to a solid support. Since immobilized enzymes are typically attached to the surface of a matrix or filler material, substrate molecules must diffuse through the surrounding medium to reach the enzyme on the support surface. As the quantity of solid support increases, the diffusion path for substrates becomes longer, thereby reducing the possibility of enzyme–substrate interactions. In other words, a higher amount of carrier surface may hinder substrate access to the enzyme, potentially limiting the reaction rate and leading to decreased enzymatic activity.[49] Additionally, enzymes may undergo conformational changes upon binding to the carrier surface. An increased amount of support can affect how the enzyme attaches to the surface, possibly leading to a loss in catalytic activity. In particular, an increase in carrier surface area may restrict access to the enzyme's active site, further inhibiting its interaction with substrates. In conclusion, the primary reason for the reduction in immobilized enzyme activity with increasing solid content includes diffusion limitations faced by the substrate in reaching the enzyme. This factor hinder efficient substrate binding and catalysis, ultimately reducing overall enzymatic activity and limiting the effective use of the support material.

pH and temperature profiles of free and immobilized POD

pH is a critical parameter that directly affects the kinetics of enzymatic reactions. Changes in pH modulate enzyme–substrate interactions by altering the ionization states of amino acid side chains and the ionic form of the substrate.[50] The optimum pH range for an enzyme is crucial for both catalytic efficiency and structural stability. In this study, the pH-dependent activity changes of free and immobilized enzyme, purified using different methods (phosphate

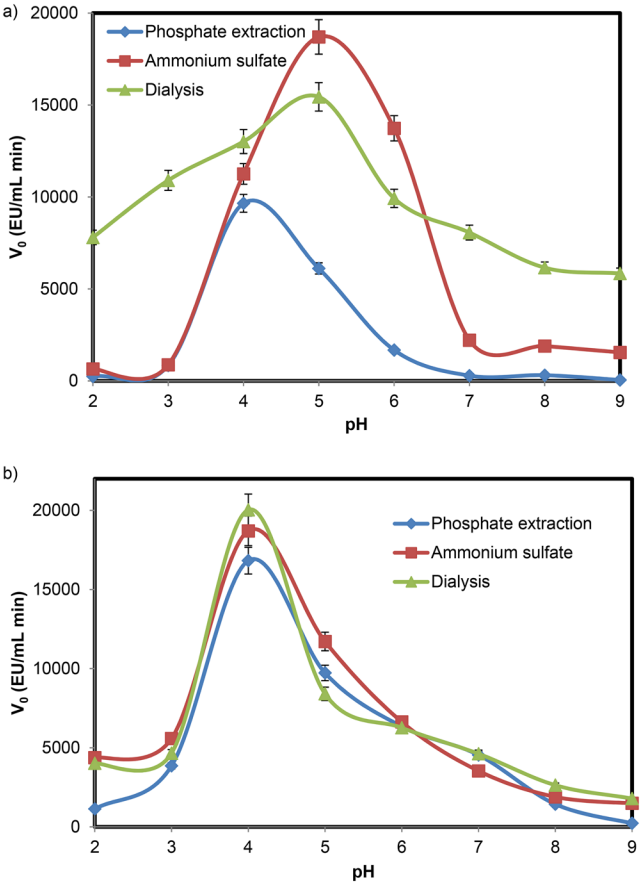

Figure 10. The changing of (a) free and (b) immobilized POD activity with pH.

extraction, ammonium sulfate precipitation, and dialysis), were extensively examined (Figure 10). For the free POD enzyme, the optimum pH after phosphate extraction was determined to be approximately 4.0. Following ammonium sulfate precipitation and dialysis, a slight shift toward more basic values (between 4.5 and 5.0) was observed. This shift may be attributed to changes in the enzyme's microenvironment, alterations in ionic strength, and removal of protein impurities during the purification process, which can affect the local environment of the active site.[38] The studies in literature show that the optimum pH values of free POD enzymes purified from various plant sources vary widely. These include sources such as corn steep liquor,[51] sweet potato tubers,[52] royal palm tree,[53] African oil palm tree,[32] *Salvia* species,[34] and horseradish,[35] with reported optimum pH values generally ranging from 3.0 to 5.0. These values are largely consistent with the findings of the present study. For the POD enzymes immobilized on the MWCNT surface, the optimum pH was preserved within the 4.0–5.0 range. A notable feature of the pH–activity profiles following immobilization was the sharper peak in activity and reduced tolerance to pH variations around the optimum. This suggests that while immobilization helps maintain the structural integrity of the enzyme, it may also narrow its pH stability range. Similarly, studies by Kim et al.[15] and Jun et al.[28] reported that PODs immobilized on carbon nanotube or composite supports exhibited enhanced pH tolerance but showed sharper activity transitions around the optimum pH.[15,28] A slight reduction in enzymatic activity was observed for the immobilized form compared to the free enzyme. This decline may be explained by restricted diffusion of the substrate to the enzyme's active site, steric hindrance caused by the carrier matrix, and possible conformational changes.[54] Studies by Alatawi et al.[9] and Monier et al.,[21] and Mohammed et al.[20] also reported minimal shifts in the optimum pH of immobilized enzymes, with preserved catalytic performance and significantly enhanced enzyme lifetimes.[9,20,21] In conclusion, the optimum pH values for both free and immobilized POD enzymes were found to be consistent with those reported in the literature. While enzyme activity increased after purification, slight activity losses were observed upon immobilization. Nevertheless, the immobilization process largely preserved the catalytic properties, offering significant advantages for industrial applications.

It should be noted that the immobilization experiments in this study were performed using POD enzyme samples that underwent three-step partial purification, including phosphate buffer extraction, ammonium sulfate precipitation, and dialysis. Each purification step significantly influenced the enzyme's optimum pH. While the crude extract showed an optimum pH of ~4.0, a slight shift toward higher pH values (4.5–5.0) was observed after ammonium sulfate precipitation and dialysis, likely due to removal of interfering compounds and changes in the enzyme's microenvironment. Despite these shifts, the immobilized enzyme preserved a similar optimum pH (4.0–5.0) range, indicating that the immobilization process did not cause any significant alterations in the enzyme's acid–base profile. The changes in optimum pH are consistent with the known sensitivity of peroxidases to purification and immobilization conditions.

The optimum temperature of an enzyme refers to the temperature range at which it exhibits its highest catalytic efficiency. This temperature corresponds to the point where the enzyme's three-dimensional structure and active site interact most effectively with the substrate. Generally, increasing temperature enhances molecular kinetic energy, thereby accelerating enzyme–substrate interactions. However, excessively high temperatures can disrupt the native conformation of proteins (denaturation), leading to a sharp decline in enzymatic activity.[55] Figure 11a,b illustrate the temperature-dependent activity changes of free and immobilized POD enzymes, respectively, following different purification steps (phosphate extraction, ammonium sulfate precipitation, and dialysis). In both graphs, the optimum temperature for free and immobilized enzymes across all purification methods was observed to be approximately 30 °C. This finding aligns with the optimum temperature (25 °C) previously reported by Gallati[35] for horseradish POD using the ABTS substrate. In both systems, free and immobilizedenzyme activity initially increased with temperature, followed by a decline beyond a certain point. This trend is consistent with the Arrhenius law: at low temperatures, reaction rates are limited, but as the temperature increases, the activation energy barrier is more easily overcome, accelerating the reaction rate. However, at high temperatures, the enzyme structure begins to denature, resulting

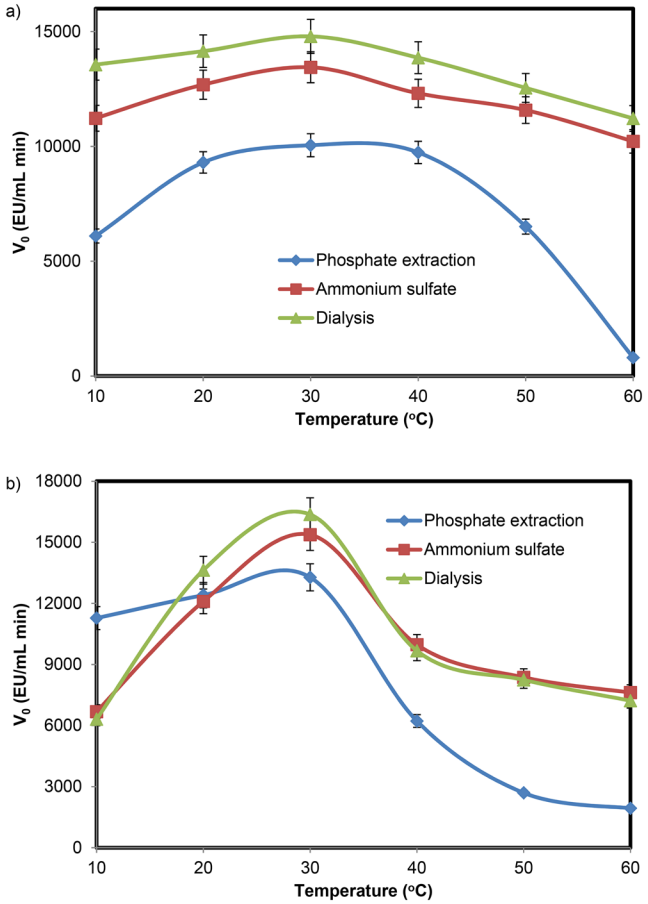

Figure 11. The changing of (a) free and (b) immobilized POD activity with temperature.

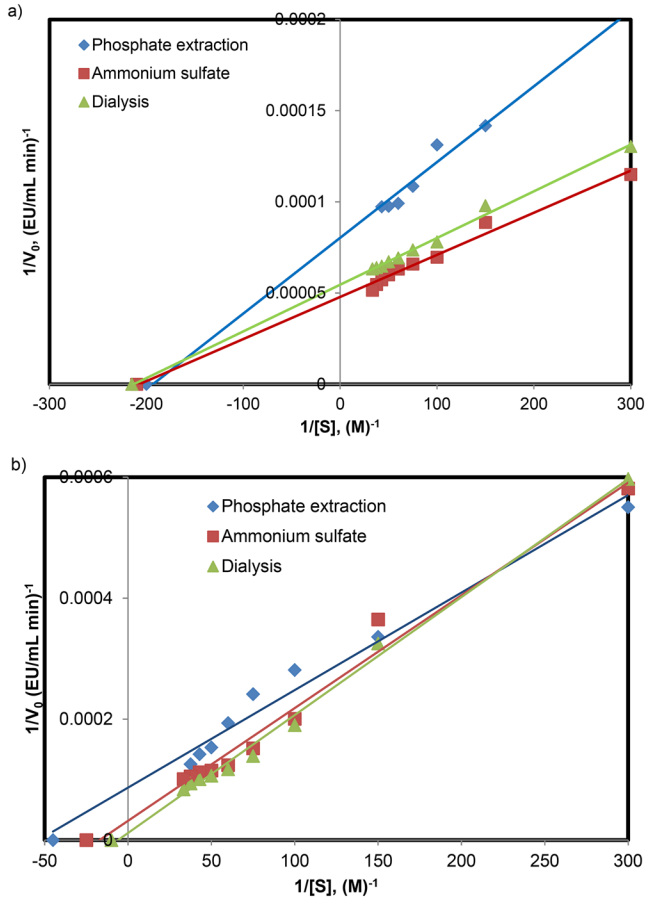

Figure 12. The plots of 1/V versus 1/[S] for (a) free and (b) immobilized POD enzyme.

in reduced activity.[56] It is known that in immobilized enzyme systems, the covalent or physical attachment of enzyme molecules to a support can provide slightly enhanced thermal tolerance. However, in this study, the optimum temperature of the immobilized enzymes did not differ significantly from that of the free form, suggesting that the immobilization method using MWCNTs did not markedly alter the enzyme's thermal stability. Previous studies have reported the optimum temperatures for PODs isolated from *S. tomentosa Miller*, *S. virgata Jacq.*, and *S. viridis L.* as 40 °C, 60 °C, and 50 °C, respectively.[34] These values are notably higher than the optimum temperature determined for celery root POD in the present study. This discrepancy may be attributed to differences in enzyme source, structural characteristics, and environmental factors. Enzymes with low optimum temperatures offer several advantages for industrial applications. Primarily, enzymes that function efficiently at lower temperatures contribute to reduced energy consumption and lower production costs.[2] Additionally, reactions carried out at lower temperatures tend to result in slower thermal denaturation. This feature is especially important for immobilized enzymes, as their reusability is a key advantage. Moreover, elevated temperatures in many industrial processes can lead to degradation of products and the formation of undesirable by-products, which can be minimized at lower temperatures.[57] In conclusion, the observation that both free and immobilized POD enzymes purified by phosphate extraction, ammonium sulfate precipitation, and dialysis exhibit an optimum temperature around 30 °C highlights their suitability for industrial biotechnology applications. Their high activity at relatively low temperatures offers significant operational and economic advantages.

Kinetic parameters of free and immobilized POD

The kinetic parameters of enzymes, V_{max}, K_M, and the V_{max}/K_M ratio, provide essential insights into their catalytic performance. V_{max} represents the maximum reaction rate achieved by the enzyme under saturated substrate conditions, while K_M reflects the enzyme's affinity for its substrate. The V_{max}/K_M ratio serves as an indicator of catalytic efficiency. Lineweaver–Burk plots (1/[S] vs. $1/V_0$) for free and immobilized POD enzymes, obtained after different purification steps (phosphate extraction, ammonium sulfate precipitation, and dialysis), are presented in Figure 12. The kinetic parameters calculated from the slope and intercepts of these plots are summarized in Table 4. For the free POD enzymes, phosphate extraction resulted in a V_{max} of 1.25×10^4 EU/mL·min and a K_M of 5×10^{-3} M. Following ammonium sulfate precipitation, V_{max} increased to 2.00×10^4 EU/mL·min, while K_M decreased to 4×10^{-3} M, indicating both an enhancement in the maximum catalytic rate and an improvement in substrate binding affinity. After dialysis, V_{max} remained constant (2.00×10^4 EU/mL·min), whereas K_M rose

Table 4. Kinetic parameters of free and immobilized PODs.

Enzymes	Purification steps	V_{max} (EU/mL min)	K_M (M)	V_{max}/K_M
Free POD	Phosphate extraction	1.25×10^{4}	5×10^{-3}	2,500,000
	Ammonium sulfate	2.00×10^{4}	4×10^{-3}	5,000,000
	Dialysis	2.00×10^{4}	6×10^{-3}	3,333,333
Immobilized POD	Phosphate extraction	1.11×10^{4}	2.22×10^{-2}	500,000
	Ammonium sulfate	3.33×10^{4}	6.67×10^{-2}	499,250
	Dialysis	1.00×10^{5}	2.00×10^{-1}	500,000

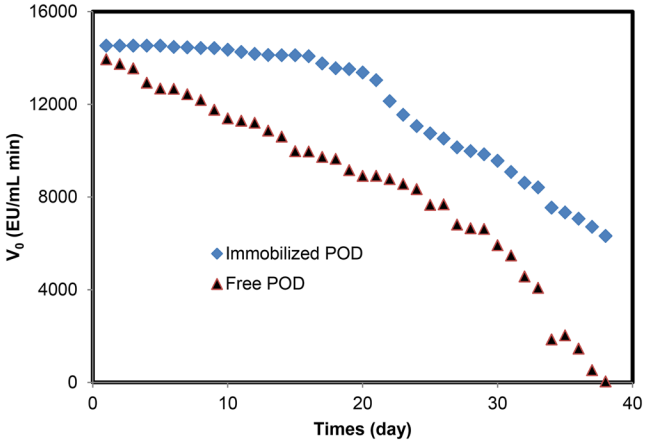

Figure 13. Time-dependent stability of free and immobilized POD enzyme.

to 6×10^{-3} M, suggesting a slight decrease in substrate affinity. Among the free enzyme preparations, ammonium sulfate precipitation yielded the highest catalytic efficiency (V_{max}/K_M= 5,000,000), implying more effective substrate interaction and accelerated reaction rates. For immobilized POD enzymes, phosphate extraction led to a V_{max} of 1.11×10^{4} EU/mL·min and a K_M of 2.22×10^{-2} M. This K_M value is approximately 4–5 times higher than those observed for the free enzymes, suggesting that immobilization reduced substrate affinity. After ammonium sulfate precipitation, V_{max} increased to 3.33×10^{4} EU/mL·min, while K_M also rose to 6.67×10^{-2} M. Post-dialysis, the highest V_{max} was recorded (1.00×10^{5} EU/mL·min), but with a substantial increase in K_M to 2.00×10^{-1} M. This trend indicates that while immobilization and purification increased the reaction rate, they simultaneously decreased the enzyme's binding affinity toward the substrate. The V_{max}/K_M ratios for the immobilized enzymes were approximately 500,000, which is about 5–10 times lower than those of the free enzymes. This suggests that immobilization reduced catalytic efficiency, likely due to partial inaccessibility of the enzyme's active site upon attachment to the support matrix, or potential conformational changes. In summary, purification, particularly ammonium sulfate precipitation, significantly improved the catalytic performance of free enzymes. Although immobilization increased the reaction rate (V_{max}), it resulted in reduced substrate affinity (as evidenced by higher K_M values) and overall catalytic efficiency. Despite reaching the highest V_{max} after dialysis, immobilized enzymes exhibited limited efficiency due to elevated K_M. These findings underscore that enzyme

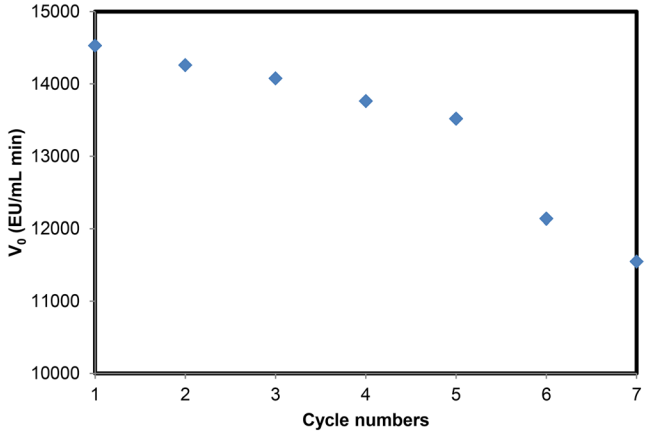

Figure 14. The reusability stability of immobilized-POD.

immobilization can substantially alter kinetic behavior and highlight the critical role of purification strategies, especially for optimizing the catalytic performance of free enzymes.

Stability and reusability of immobilized POD

Figure 13 illustrates the change in enzymatic activity of both free and immobilized POD over a 38-day period. Initially, both enzyme forms exhibit high catalytic activity. However, while the free POD shows a marked decline after day 20 and nearly loses all activity by day 35, the immobilized enzyme maintains a relatively stable profile. Notably, the immobilized POD retains a significant level of activity (~7000 EU/mL·min) even at day 38. This finding suggests that immobilization confers increased resistance to environmental stressors and helps preserve the structural integrity of the enzyme. Consistent with the literature, enzyme immobilization enhances conformational stability and improves resistance against denaturation, proteolytic degradation, and pH fluctuations.[1,2] Furthermore, immobilized enzymes exhibit improved storage and operational stability, leading to extended shelf life and reduced activity loss during transportation and handling. These results indicate that immobilized enzyme systems offer superior stability, reliability, and longevity compared to free enzymes, and thus present a considerable advantage for industrial and biotechnological applications.

Figure 14 illustrates the reusability stability of immobilized POD over seven consecutive cycles. The enzyme initially exhibited an activity of approximately 14,600 EU/mL·min, which gradually decreased to around 11,600 EU/mL·min by the seventh cycle. The relatively low loss of activity during the first five cycles indicates a certain degree of structural stability and operational durability, suggesting that the immobilization method effectively enables the enzyme for multiple reuses. This is a promising feature for industrial applications, where reusability is crucial for cost-effectiveness and sustainability. The observed decline in activity may be attributed to potential enzyme leaching from the support matrix, substrate diffusion limitations, or partial structural denaturation. Notably, a more pronounced decrease in activity was observed in the sixth and seventh cycles, implying that prolonged reuse might

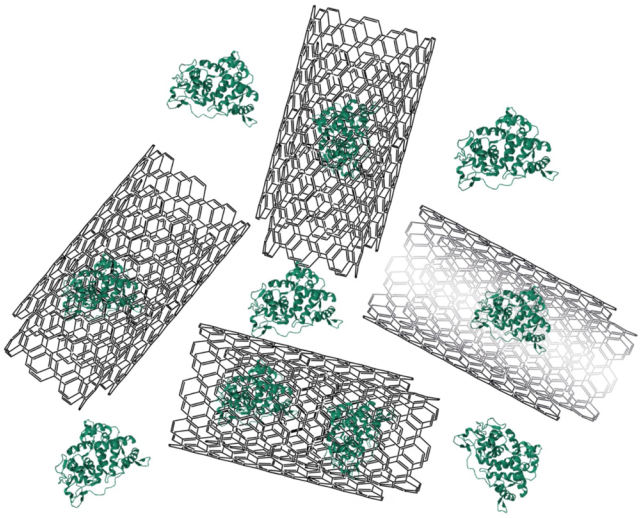

Figure 15. Immobilization of POD on the surface, intertubular regions and pores of MWCNT.

necessitate re-immobilization. Overall, the immobilized enzyme demonstrates acceptable reusability, highlighting its potential for repeated applications in biocatalytic processes.

Comparison with literature and proposed mechanism of immobilization

The reusability profile of immobilized POD in this work aligns closely with trends reported across various studies. For instance, Aldhahri et al.[58] found that HRP immobilized on modified chitosan beads retained ~65% activity after 5 cycles, which is comparable to the ~90% activity retained after 5 cycles in the present study. Azevedo et al.[59] reported 4.5-fold increased storage stability for peroxidase on surface-oxidized MWCNTs compared to free enzyme, reinforcing our observation of enhanced operational durability attributable to hydrogen-bond mediated immobilization. In the work by Jun et al.,[28] immobilized jicama peroxidase on BP/PVA-MWCNT membranes exhibited improved operational and storage stability, along with high enzyme loading (~217 mg/g) and ~80% residual activity after repeated uses, consistent with strengthening of enzyme-support interactions in our system. Bila et al.[60] and Lee et al.[29] demonstrated that immobilized HRP on carboxylated MWCNTs maintained oxidative activity across a wide pH range (4–9), similar to our enzyme which retained >70% activity under varied pH conditions. Bilal et al.[60] showed HRP on MWCNT-chitosan-magnetic hybrids preserved around 80% activity after 10 cycles and 20 days of storage, emphasizing that extended reusability and stability are achievable with composite supports. In line with this, a Fe_3O_4–MWCNT peroxidase-mimicking catalyst maintained "no obvious loss" of activity over multiple uses in dye removal,[61] echoing our findings of a plateau in activity loss during early reuse cycles. A covalent immobilization study on reduced graphene oxide by Vineh et al.[62] reported 70% retained activity after 10 cycles and ~97% storage activity after 35-day which mirrors our results in demonstrating both operational and long-term stability. Similarly, Fe_3O_4–MWCNT catalysts in Fenton-like reactions showed broad pH tolerance (1–10) and rapid magnetic recovery with negligible activity loss over reuses,[61] supporting the robust performance exhibited by the POD-MWCNT system here. Finally, results align with broader conclusions in reviews on enzyme–CNT composites, which highlight that carbon nanomaterials enhance enzyme stability and reusability through strong physical and chemical interactions.

In line with the above explanations, Figure 15 illustrates the immobilization of POD on the surface of MWCNTs, in the intertubular regions, and within the mesoporous interiors of the tubes. The interactions here are physical, especially van der Waals type interactions.

Conclusions

In this study, POD was successfully extracted and concentrated from celery root and immobilized onto MWCNTs. The immobilization conditions were optimized in terms of time and support amount, with optimal activity observed at 300 minutes. Characterization analyses (BET, FTIR, SEM/EDX, TGA, TEM) confirmed the successful attachment of the enzyme to the MWCNT surface. BET analysis demonstrated a reduction in surface area from 275 to 197 m^2/g, indicating effective enzyme coating. FTIR spectra revealed distinct protein-related functional groups, while SEM/EDX and TEM analyses showed morphological changes and elemental compositions consistent with enzyme presence, including Fe as a POD cofactor. Thermal analysis demonstrated altered degradation patterns, supporting the integration of the enzyme into the nanotube structure. Kinetic studies showed that although V_{max} values were retained or increased, K_M values rose significantly, indicating reduced substrate affinity likely due to diffusional or steric hindrances. Despite this, the immobilized enzyme maintained high catalytic activity under optimal pH (4.0–5.0) and temperature (30 °C) conditions, and exhibited enhanced storage and reusability profiles, retaining activity over 38 days and multiple usage cycles. These findings underscore the potential of POD-MWCNT systems as robust and reusable biocatalysts for environmental and industrial applications, combining the advantages of nanomaterials with enzyme functionality.

Disclosure statement

No potential conflict of interest was reported by the author(s).

Funding

This work was supported by Balikesir Üniversitesi (BAP 2020/102).

References

[1] Datta, S.; Christena, L. R.; Rajaram, Y. R. S. Enzyme Immobilization: An Overview on Techniques and Support Materials. *3 Biotech* **2013**, *3*, 1–9. DOI: 10.1007/s13205-012-0071-7.

[2] Sheldon, R. A.; van Pelt, S. Enzyme Immobilisation in Biocatalysis: Why, What and How. *Chem. Soc. Rev.* **2013**, *42*, 6223–6235. DOI: 10.1039/c3cs60075k.

[3] Kuang, G.; Wang, Z.; Bilal, M.; Wang, Z.; Feng, Y.; Du, Y.; Cui, J. Metal–Organic Frameworks: A Potential Platform from Enzyme Immobilization to Mimetic Enzyme. *Aggregate* **2025**, *6*, e724. DOI: 10.1002/agt2.724.

[4] Wang, R.; Chang, Y.; Li, J.; Yang, S.; Zhu, T.; Bi, Y.; Cui, J. Carbonic Anhydrase-Embedded ZIF-8 Membrane Reactor with Improved Recycling and Stability for Efficient CO2 Capture. Int. J. Biol. Macromol. 2024, 280, 136083. DOI: 10.1016/j.ijbiomac.2024.136083.[39353523]

[5] Wang, Z.; Wang, R.; Geng, Z.; Luo, X.; Jia, J.; Pang, S.; Fan, X.; Bilal, M.; Cui, J. Enzyme Hybrid Nanoflowers and Enzyme@ Metal–Organic Frameworks Composites: Fascinating Hybrid Nanobiocatalysts. *Crit. Rev. Biotechnol.* **2024**, *44*, 674–697. DOI: 10.1080/07388551.2023.2189548.

[6] Du, Y.; Zhao, L.; Geng, Z.; Huo, Z.; Li, H.; Shen, X.; Peng, X.; Yan, R.; Cui, J.; Jia, S. Construction of Catalase@Hollow Silica Nanosphere: Catalase with Immobilized but Not Rigid State for Improving Catalytic Performances. *Int. J. Biol. Macromol.* **2024**, *263*, 130381. DOI: 10.1016/j.ijbiomac.2024.130381.

[7] Zhong, L.; Wang, Z.; Ye, X.; Cui, J.; Wang, Z.; Jia, S. Molecular Simulations Guide Immobilization of Lipase on Nest-like ZIFs with Regulatable Hydrophilic/Hydrophobic Surface. *J. Colloid Interface Sci.* **2024**, *667*, 199–211. DOI: 10.1016/j.jcis.2024.04.075.

[8] Veitch, N. C. Horseradish Peroxidase: A Modern View of a Classic Enzyme. *Phytochemistry* **2004**, *65*, 249–259. DOI: 10.1016/j.phytochem.2003.10.022.

[9] Alatawi, W. A.; Altowairqi, M. H.; Khan, M. I. Immobilization of Horseradish Peroxidase on Nylon-6 and Its Application in Phenol Removal. *Molecules* **2020**, *25*, 1679. DOI: 10.3390/molecules25071679.

[10] Barbosa, O.; Ariza, C.; Ortiz, C.; Torres, R.; Fernández-Lafuente, R. Effect of the Immobilization Protocol on the Properties of Peroxidase Immobilized on Poly-Aniline Coated Magnetic Nanoparticles. *Process Biochem* .**2012**, *47*, 2130–2137. DOI: 10.1016/j.procbio.2012.07.030.

[11] Fernandes, K. F.; Filho, M. R.; Robles, J. Immobilization of Horseradish Peroxidase onto Polyaniline Activated with Glutaraldehyde. *Process Biochem.* **2003**, *39*, 625–632. DOI: 10.1016/S0032-9592(03)00148-6.

[12] Gomez, J. L. C.; Ortega, M. T.; Hernández, L. C.; Ortiz-Ortega, A. Phenol Removal by Horseradish Peroxidase Immobilized on Aminopropyl Glass Beads. *Enzyme Microb. Technol.* **2006**, *39*, 498–503. DOI: 10.1016/j.enzmictec.2005.11.048.

[13] Marchis, T.; Cerrato, G.; Magnacca, G.; Crocellà, V.; Laurenti, E. Immobilization of Soybean Peroxidase on Aminopropyl Glass Beads: Structural and Kinetic Studies. *Biochem. Eng. J.* **2012**, *67*, 28–34. DOI: 10.1016/j.bej.2012.05.002.

[14] Jun, L. Y.; Mubarak, N. M.; Yon, L. S.; Bing, C. H.; Khalid, M.; Jagadish, P.; Abdullah, E. C. Immobilization of Peroxidase on Functionalized MWCNTs-Buckypaper/Polyvinyl Alcohol Nanocomposite Membrane. *Sci. Rep.* **2019**, *9*, 2215. DOI: 10.1038/s41598-019-39621-4.

[15] Kim, J.; Grate, J. W.; Wang, P. Nanostructures for Enzyme Stabilization. *Chem. Eng. Sci.* **2009**, *64*, 1375–1386. DOI: 10.1016/j.ces.2008.10.027.

[16] Kim, H. J.; Suma, Y.; Lee, S. H.; Kim, J.-A.; Kim, H. S. Immobilization of Horseradish Peroxidase onto Clay Minerals Using Soil Organic Matter for Phenol Removal. *J. Mol. Catal. B Enzym.* **2012**, *83*, 8–15. DOI: 10.1016/j.molcatb.2012.06.012.

[17] Magri, M. L.; Loustau, M. D. L. N.; Miranda, M. V.; Cascone, O. Immobilisation of Soybean Seed Coat Peroxidase on Its Natural Support for Phenol Removal from Wastewater. *Biocatal. Biotransform.* **2007**, *25*, 98–102. DOI: 10.1080/10242420601142992.

[18] Melo, M. N.; Pereira, F. M.; Rocha, M. A.; Ribeiro, J. G.; Diz, F. M.; Monteiro, W. F.; Ligabue, R. A.; Severino, P.; Fricks, A. T. Immobilization and Characterization of Horseradish Peroxidase into Chitosan and Chitosan/PEG Nanoparticles: A Comparative Study. *Process Biochem.* **2020**, *98*, 160–171. DOI: 10.1016/j.procbio.2020.08.007.

[19] Mohamed, S. A.; Darwish, A. A.; El-Shishtawy, R. M. Immobilization of Horseradish Peroxidase on Activated Wool. *Process Biochem.* **2013**, *48*, 649–655. DOI: 10.1016/j.procbio.2013.03.002.

[20] Mohamed, S. A.; Al-Harbi, M. H.; Almulaiky, Y. Q.; Ibrahim, I. H.; El-Shishtawy, R. M. Immobilization of Horseradish Peroxidase on Fe_3O_4 Magnetic Nanoparticles. *Electron. J. Biotechnol.* **2017**, *27*, 84–90. DOI: 10.1016/j.ejbt.2017.03.010.

[21] Monier, M.; Ayad, D. M.; Wei, Y.; Sarhan, A. A. Immobilization of Horseradish Peroxidase on Modified Chitosan Beads. *Int. J. Biol. Macromol.* **2010**, *46*, 324–330. DOI: 10.1016/j.ijbiomac.2009.12.018.

[22] Nicolini, J. V.; Ferraz, H. C.; de Resende, N. S. Immobilization of Horseradish Peroxidase on Titanate Nanowires for Biosensing Application. *J. Appl. Electrochem.* **2016**, *46*, 17–25. DOI: 10.1007/s10800-015-0907-z.

[23] Rojas-Melgarejo, F.; Rodríguez-López, J. N.; García-Cánovas, F.; García-Ruiz, P. A. Immobilization of Horseradish Peroxidase on Cinnamic Carbohydrate Esters. *Process Biochem.* **2004**, *39*, 1455–1464. DOI: 10.1016/S0032-9592(03)00276-0.

[24] Shi, P.; Wu, Z.; Liu, Y.; Zhang, G.; Zhang, C. Immobilization of Horseradish Peroxidase on Metal-Organic Framework to Improve Enzyme Activity for Enhanced Chemodynamic Therapy. *J. Inorg. Biochem.* **2024**, *250*, 112394. DOI: 10.1016/j.jinorgbio.2023.112394.

[25] Varamini, M.; Zamani, H.; Hamedani, H.; Namdari, S.; Rastegari, B. Immobilization of Horseradish Peroxidase on Lysine-Functionalized Gum Arabic-Coated Fe_3O_4 Nanoparticles for Cholesterol Determination. *Prep. Biochem. Biotechnol.* **2022**, *52*, 737–747. DOI: 10.1080/10826068.2021.1992780.

[26] Doğan, E. E.; Tokcan, P.; Kizilduman, B. K. Storage of Hydrogen in Activated Carbons and Carbon Nanotubes. *Adv. Mater. Sci.* **2018**, *18*, 5–16. DOI: 10.1515/adms-2017-0045.

[27] Doğan, Z. S.; Doğan, E. E.; Bicil, Z.; Koçer Kizilduman, B. The Effect of Li-Doping and Doping Methods to Hydrogen Storage Capacities of Some Carbonaceous Materials. *Fuel* **2025**, *396*, 135280. DOI: 10.1016/j.fuel.2025.135280.

[28] Jun, H.; Son, J.; Lee, Y. C.; Hong, W. H. Jicama Peroxidase Immobilization on Functionalized MWCNT/PVA Composite Membrane and Its Application. *Int. J. Biol. Macromol.* **2019**, *123*, 725–733. DOI: 10.1016/j.ijbiomac.2018.11.105.

[29] Lee, Y.-M.; Kwon, O.-Y.; Yoon, Y.-J.; Ryu, K. Immobilization of Horseradish Peroxidase on Multi-Wall Carbon Nanotubes and Its Electrochemical Properties. *Biotechnol. Lett.* **2006**, *28*, 39–43. DOI: 10.1007/s10529-005-9685-8.

[30] Li, S.; Liu, B.; Zhang, Y.; Cao, Y. A Recyclable HRP-Immobilized Cordierite-Based Catalyst for Phenol Removal. *Appl. Surf. Sci.* **2017**, *423*, 1159–1168. DOI: 10.1016/j.apsusc.2017.06.224.

[31] Yalçinkaya, F. N.; Doğan, M.; Bicil, Z.; Koçer Kizilduman, B. Effect of Functionalization and Li-Doping Methods to Hydrogen Storage Capacities of MWCNTs. *Fuel* **2024**, *372*, 132274. DOI: 10.1016/j.fuel.2024.132274.

[32] Sakharov, I. Y.; Vesga Blanco, M. K.; Sakharova, I. V. Substrate Specificity of African Oil Palm Tree Peroxidase. *Biochemistry.* **2002**, *67*, 1043–1047. DOI: 10.1023/A:1020534321683.

[33] Çam, Ş.; Doğan, M.; Beyli, P. T.; Doğan, S.; Bicil, Z.; Kızılduman, B. K. Immobilization, Optimization, Characterization and Kinetic Properties of Polyphenol Oxidase to Multi-Walled Carbon Nanotube. *Prep. Biochem. Biotechnol.* **2025**, 1–14. DOI: 10.1080/10826068.2025.2498460.

[34] Doğan, S.; Turan, P.; Doğan, M.; Arslan, O.; Alkan, M. Variations of Peroxidase Activity among Salvia Species. *J. Food Eng.* **2007**, *79*, 375–382. DOI: 10.1016/j.jfoodeng.2006.02.001.

[35] Gallati, H. Horseradish Peroxidase: A Study of the Kinetics and the Determination of Optimal Reaction Conditions, Using Hydrogen Peroxide and 2,2'-Azinobis(3-Ethylbenzthiazoline-6-S ulfonic Acid) (ABTS) as Substrates. *J. Clin. Chem. Clin. Biochem.* **1979**, *17*, 1–7.

[36] Doğan, S.; Doğan, M. Determination of Kinetic Properties of Polyphenol Oxidase from Thymus (Thymus Longicaulis Subsp. chaubardii Var. chaubardii). *Food Chem.* **2004**, *88*, 69–77. DOI: 10.1016/j.foodchem.2003.12.025.

[37] Wang, H.; Li, S.; Li, J.; Zhong, L.; Cheng, H.; Ma, Q. Immobilized Polyphenol Oxidase: Preparation, Optimization and Oxidation of

Phenolic Compounds. *Int. J. Biol. Macromol.* **2020**, *160*, 233–244. DOI: 10.1016/j.ijbiomac.2020.05.079.
[38] Doğan, M.; Bicil, Z.; Koçer Kizilduman, B.; Turhan, Y.; Pehlivan, F. Functionalization and Metal Doping of MWCNTs for Hydrogen Storage. *J. Energy Storage* **2025**, *122*, 116653. DOI: 10.1016/j.est.2025.116653.
[39] Bayne, L.; Ulijn, R. V.; Halling, P. J. Effect of Pore Size on the Performance of Immobilised Enzymes. *Chem. Soc. Rev.* **2013**, *42*, 9000–9010. DOI: 10.1039/c3cs60270b.
[40] Baltacıoğlu, H.; Coruk, K. S. Determination of Conformational Changes of Polyphenol Oxidase and Peroxidase in Peach Juice during Mild Heat Treatment Using FTIR Spectroscopy Coupled with Chemometrics. *Int. J. of Food Sci. Tech.* **2021**, *56*, 2915–2925. DOI: 10.1111/ijfs.14930.
[41] Çakir, Ü.; Doğan, M.; Kizilduman, B. K.; Bïcïl, Z. Functionalized and Schiff Base Based Multi Walled Carbon Nanotubes for Hydrogen Storage. *J. Alloys Compd.* **2025**, *1010*, 177290. DOI: 10.1016/j.jallcom.2024.177290.
[42] Çakır, Ü.; Kestel, F.; Koçer Kızılduman, B.; Bicil, Z.; Doğan, M. Multi Walled Carbon Nanotubes Functionalized by Hydroxyl and Schiff Base and Their Hydrogen Storage Properties. *Diam. Relat. Mater* **2021**, *120*, 108604. DOI: 10.1016/j.diamond.2021.108604.
[43] Cristóvão, R. O.; Almeida, M. R.; Barros, M. A.; Nunes, J. C. F.; Boaventura, R. A. R.; Loureiro, J. M.; Faria, J. L.; Neves, M. C.; Freire, M. G.; Ebinuma-Santos, V. C.; et al. Development and Characterization of a Novel L-Asparaginase/MWCNT Nanobioconjugate. *RSC Adv.* **2020**, *10*, 31205–31213. DOI: 10.1039/d0ra05534d.
[44] Lee, C.; Lee, S.-Y. Hemin-Bound Cysteinyl Bolaamphiphile Selfassembly as a Horseradish Peroxidase-Mimetic Catalyst. *RSC Adv.* **2017**, *7*, 38989–38997. DOI: 10.1039/C7RA06547G.
[45] Rodrigues, R. C.; Ortiz, C.; Berenguer-Murcia, Á.; Torres, R.; Fernández-Lafuente, R. Modifying Enzyme Activity and Selectivity by Immobilization. *Chem. Soc. Rev.* **2013**, *42*, 6290–6307. DOI: 10.1039/c2cs35231a.
[46] Zhang, Y.; Ge, J.; Liu, Z. Enhanced Activity of Immobilized or Chemically Modified Enzymes. *ACS Catal.* **2015**, *5*, 4503–4513. DOI: 10.1021/acscatal.5b00996.
[47] Eldin, M. S. M.; Mita, D. G. Immobilized Enzymes: Strategies for Overcoming the Substrate Diffusion- Limitation Problem. *CBIOT.* **2014**, *3*, 207–217. DOI: 10.2174/2211550103031409181147 37.
[48] Bolivar, J. M.; Nidetzky, B. On the Relationship between Structure and Catalytic Effectiveness in Solid Surface-Immobilized Enzymes: Advances in Methodology and the Quest for a Single-Molecule Perspective. *Biochim. Biophys. Acta. Proteins Proteom.* **2020**, *1868*, 140333. DOI: 10.1016/j.bbapap.2019.140333.
[49] Montanier, C. Y.; Fanuel, M.; Rogniaux, H.; Ropartz, D.; Guilmi, A.-M. D.; Bouchoux, A. Changing Surface Grafting Density Has an Efect on the Activity of Immobilized Xylanase towards Natural Polysaccharides. *Sci. Rep.* **2019**, *9*, 5763. DOI: 10.1038/s41598-019-42206-w.
[50] Doğan, S.; Turan, P.; Doğan, M. Some Kinetic Properties of Polyphenol Oxidase from Thymbra Spicata L. var. spicata. *Process Biochem.* **2006**, *41*, 2379–2385. DOI: 10.1016/j.procbio.2006.06.013.
[51] Gray, J. S. S.; Montgomery, R. Purification and Characterization of a Peroxidase from Corn Steep Water. *J. Agric. Food Chem.* **2003**, *51*, 1592–1601. DOI: 10.1021/jf025883n.
[52] Leon, J.; Alpeeva, I. S.; Chubar, T. A.; Galaev, I.; Csoregi, E.; Sakharov, I. Purification and Substrate Specificity of Peroxidase from Sweet Potato Tubers. *Plant Sci.* **2002**, *163*, 1011–1019. DOI: 10.1016/S0168-9452(02)00275-3.
[53] Sakharov, I. Y.; Vesga, M. K.; Galaev, I. Y.; Sakharova, I. V.; Pletjushkina, O. Y. Peroxidase from Leaves of Royal Palm Tree Roystonea Regia: Purification and Some Properties. *Plant Sci.* **2001**, *161*, 853–860. DOI: 10.1016/S0168-9452(01)00466-6.
[54] Zhang, C.; Cai, X. Immobilization of Horseradish Peroxidase on Fe_3O_4/Nanotubes Composites for Biocatalysis-Degradation of Phenol. *Compos. Interfaces* **2019**, *26*, 379–396. DOI: 10.1080/09276440.2018.1504265.
[55] Bisswanger, H. *Enzyme Kinetics: Principles and Methods*, 3rd ed.; Wiley-VCH: Weinheim, Germany, **2014**.
[56] Nelson, D. L.; Cox, M. M. *Lehninger Principles of Biochemistry*, 7th ed.; W.H. Freeman and Company: New York, **2017**.
[57] Klibanov, A. M. Stabilization of Enzymes against Thermal Inactivation. *Adv. Appl. Microbiol.* **1983**, *29*, 1–28. DOI: 10.1016/S0065-2164(08)70352-6.
[58] Aldhahri, M. M.; Almulaiky, Y. Q.; El-Shishtawy, R. M.; Al-Shawafi, W.; Alngadh, A.; Maghrabi, R. Facile Immobilization of Enzyme via Co-Electrospinning: A Simple Method for Enhancing Enzyme Reusability and Monitoring an Activity-Based Organic Semiconductor. *ACS Omega.* **2018**, *3*, 6346–6350. DOI: 10.1021/acsomega.8b00366.
[59] Azevedo, R. M.; Costa, J. B.; Serp, P.; Loureiro, J. M.; Faria, J. L.; Silva, C. G.; Tavares, A. P. A Strategy for Improving Peroxidase Stability via Immobilization on Surface Modified Multi-Walled Carbon Nanotubes. *J. Chem. Technol. Biotechnol.* **2015**, *90*, 1570–1578. DOI: 10.1002/jctb.4698.
[60] Bilal, M.; Degorska, O.; Szada, D.; Rybarczyk, A.; Zdarta, A.; Kaplon, M.; Zdarta, J.; Jesionowski, T. Support Materials of Organic and Inorganic Origin as Platforms for Horseradish Peroxidase Immobilization: Comparison Study for High Stability and Activity Recovery. *Molecules* **2024**, *29*, 710. DOI: 10.3390/molecules29030710.
[61] Wang, H.; Jiang, H.; Wang, S.; Shi, W.; He, J.; Liu, H.; Huang, Y. Fe_3O_4–MWCNT Magnetic Nanocomposites as Efficient Peroxidase Mimic Catalysts in a Fenton-like Reaction for Water Purification without pH Limitation. *RSC Adv.* **2014**, *4*, 45809–45815. DOI: 10.1039/C4RA07327D.
[62] Vineh, M. B.; Saboury, A. A.; Poostchi, A. A.; Rashidi, A. M.; Parivar, K. Stability and Activity Improvement of Horseradish Peroxidase by Covalent Immobilization on Functionalized Reduced Graphene Oxide and Biodegradation of High Phenol Concentration. *Int. J. Biol. Macromol.* **2018**, *106*, 1314–1322. DOI: 10.1016/j.ijbiomac.2017.08.133.